International Journal of Heat and Mass Transfer 52 (2009) 4683–4688

Contents lists available at ScienceDirect

International Journal of Heat and Mass Transfer

journal homepage: www.elsevier.com/locate/ijhmt

Geometric optimization of T-Y-shaped cavity according to Constructal design

Giulio Lorenzini [a,*], Luiz Alberto Oliveira Rocha [b]

[a] Department of Agricultural Economics and Engineering, Alma Mater Studiorum – University of Bologna, viale Giuseppe Fanin No. 50, 40127 Bologna, Italy
[b] Federal University of Rio Grande, School of Engineering, Cx.P. 474, Rio Grande, RS 96201-900, Brazil

ARTICLE INFO

Article history:
Received 13 March 2009
Accepted 24 June 2009
Available online 24 July 2009

Keywords:
Constructal design
Enhanced heat transfer
Fins
Optimization

ABSTRACT

This paper applies Constructal design to optimize the geometry of a T-Y-shaped cavity that penetrates into a solid conducting wall. The objective is to minimize the global thermal resistance between the solid and the cavity. There is uniform heat generation on the solid wall. The total volume and the cavity volume are fixed, but the geometric lengths of the T-Y-shaped cavity can vary. The shape of T-Y cavity is optimal under the following conditions: it penetrates the conducting wall almost completely, the shape of the area of the solid inserted into the cavity is long enough to cross completely the T-Y-shaped cavity (ending at the coordinate $\tilde{y} = 0$), and this area is 14% of the total area occupied by the body and the T-Y-shaped cavity. The results also show that the optimal T-Y-shaped cavity performs approximately 108% better when compared with an optimal C-shaped cavity.

1. Introduction

This paper reports numerically the optimization of the global performance of a T-Y-shaped cavity that intrudes into a solid conducting wall. The optimization is conducted by applying Constructal design. According to this method "the flow geometry is malleable and it is deduced from a principle of global performance maximization subjected to global constraints" [1,2]. This method is based on Constructal theory: "the view that flow configuration (geometry, design) can be reasoned on the basis of a principle of configuration, generation and evolution in time toward greater global flow access in systems that are free to morph" [3].

Many applications of Constructal theory to generate configuration in nature, and engineering have been reviewed recently [4]. This reference shows how natural configuration – river basins, turbulence, animal design, crack in solids, earth climate, etc., can be predicted by principle. The same principle can be applied in the engineering realm: packing of electronics, fuel cells, tree networks for transport of people, goods and information, etc.

The heat transfer field has dedicated great attention to the study of fins arrays [5,6]. In the other side, open cavities are the regions formed between adjacent fins and they may represent essential promoters of nucleate boiling: see, for example, the Vapotron effect [7–9] that occurs as a consequence of the thermal interaction between a non-isothermal finned surface and a fluid locally subjected to a transient change of phase. The significance of fins and cavities is recognized by the application of Constructal method in the pursuit of best shapes of assembly of fins [10,11] and cavities [12–14].

In this paper, we apply Constructal design to optimize the geometry of the T-Y-shaped cavity. According to Constructal design, the cavity shape is free to change subject to volume constraints in the pursuit of maximal global performance. The global performance indicator is the global thermal resistance between the volume of the entire system (cavity and solid) and the surroundings. For simplicity and clarity, we consider two-dimensional bodies: the square solid and the T-Y-shaped intrusion with variable geometric lengths.

To conclude this section, it is extremely important to mention how this research and, in general, how the new study area of Constructal cavities can result strategic in the design of surface geometries for enhanced vapour generation.

In fact, the use of boiling to augment heat removal from hot surfaces has widely proved to be one of the more effective techniques, especially when associated to extended surfaces (e.g. Vapotron effect) or to cavities, able to improve the thermal performances of the systems investigated.

No doubt, then, that the use of Constructal optimization to design heat exchanging modules interested by a phase change in the coolant can add a significant contribution in the way of ever more performing heat exchangers.

2. Mathematical model

Consider the conducting body shown in Fig. 1. The configuration is two-dimensional, with the third dimension (W) sufficiently long in comparison with the height H and the length L of the volume occupied by the body. There is a T-Y-shaped cavity intruded in

* Corresponding author. Tel.: +39 051 2096186; fax: +39 051 2096178.
E-mail addresses: giulio.lorenzini@unibo.it (G. Lorenzini), dfsrocha@furg.br (L.A.O. Rocha).

0017-9310/$ - see front matter © 2009 Elsevier Ltd. All rights reserved.
doi:10.1016/j.ijheatmasstransfer.2009.06.020

Nomenclature

a	dimensionless parameter, Eq. (20)
A	area [m^2]
h	heat transfer coefficient [$W\,m^{-2}\,K^{-1}$]
H	height [m]
k	body thermal conductivity [$W\,m^{-1}\,K^{-1}$]
L	length [m]
q	heat current [W]
t	thickness [m]
T	temperature [K]
V	volume [m^3]
W	width [m]

Greek symbols

θ	dimensionless temperature, Eq. (9)
ϕ	area fraction
ψ	auxiliary area fraction

Subscripts

aux	auxiliary
c	cavity
m	single optimization
mm	double optimization
mmm	triple optimization
o	optimal
oo	twice optimized
ooo	three times optimized

Superscript

(~)	dimensionless variables, Eq. (10)

the body. The solid is isotropic with the constant thermal conductivity k. It generates heat uniformly at the volumetric rate q''' (W/m^3). The outer surfaces of the heat generating body are perfectly insulated. The generated heat current ($q'''A$) is removed by convection heat transfer through the cavity walls. The heat transfer coefficient h is uniform over all the exposed surfaces.

The objective of the analysis is to determine the optimal geometry (H_0/L_0, H_1/L_1, H_2/L_2) that is characterized by the minimum global thermal resistance $(T_{max} - T_\infty)/(q'''A)$. According to Constructal design [3], this optimization can be subjected to two constraints, namely, the total area constraint,

$$A = HL \tag{1}$$

and the cavity area constraint,

$$A_c = 2L_1H_1 + (H_2 - H_1/2)L_2 - H_0L_0 \tag{2}$$

The area of the solid inserted into the cavity is also considered constraint

$$A_0 = H_0L_0 \tag{3}$$

as well as the auxiliary area

$$A_{aux} = 2L_1H_2 + L_1H_1 \tag{4}$$

Eqs. (2)–(4) can be expressed as the cavity fraction

$$\phi_c = A_c/A \tag{5}$$

the area of the solid inserted into the cavity fraction

$$\phi_0 = A_0/A \tag{6}$$

and the auxiliary fraction area

$$\psi = A_{aux}/A \tag{7}$$

The analysis that delivers the global thermal resistance as a function of the geometry consists of solving numerically the heat conduction equation along the solid region,

$$\frac{\partial^2\theta}{\partial\tilde{x}^2} + \frac{\partial^2\theta}{\partial\tilde{y}^2} + 1 = 0 \tag{8}$$

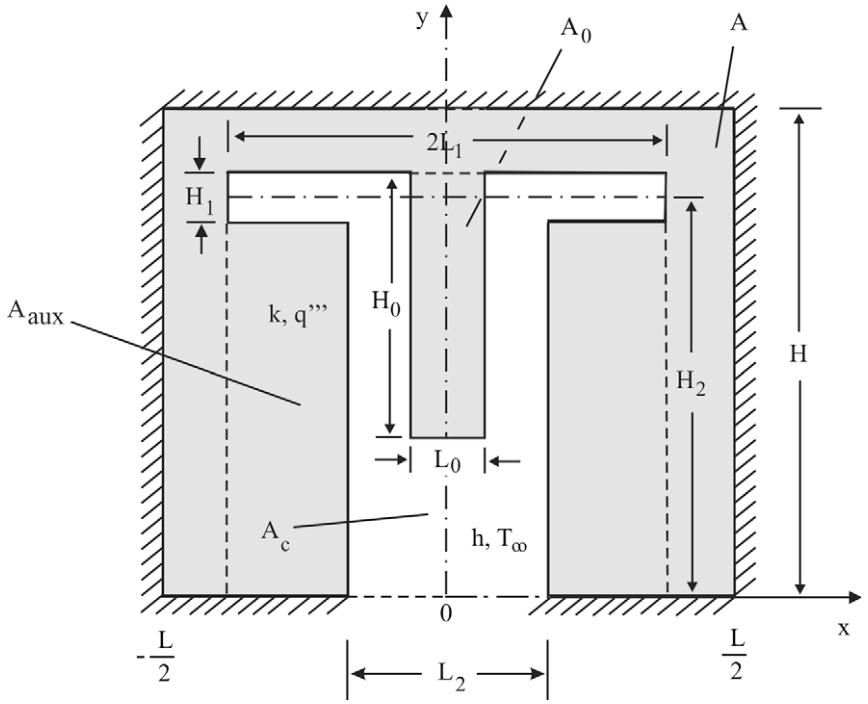

Fig. 1. Y-T-shaped cavity.

where the dimensionless variables are

$$\theta = \frac{T - T_\infty}{q''' A/K} \tag{9}$$

and

$$\tilde{x}, \tilde{y}, \tilde{H}_0, \tilde{L}_0, \tilde{H}_1, \tilde{L}_1, \tilde{H}_2, \tilde{L}_2, \tilde{H}, \tilde{L} = \frac{x, y, H_0, L_0, H_1, L_1, H_2, L_2, H, L}{A^{1/2}} \tag{10}$$

The outer surfaces are insulated and their boundary conditions are

$$\frac{\partial\theta}{\partial\tilde{x}} = 0 \quad \text{at} \quad \tilde{x} = -\frac{\tilde{L}}{2} \quad \text{or} \quad \tilde{x} = \frac{\tilde{L}}{2} \quad \text{and} \quad 0 \leqslant \tilde{y} \leqslant \tilde{H} \tag{11}$$

$$\frac{\partial\theta}{\partial\tilde{y}} = 0 \quad \text{at} \quad \tilde{y} = 0 \quad \text{and} \quad -\frac{\tilde{L}}{2} \leqslant \tilde{x} \leqslant -\frac{\tilde{L}_2}{2} \quad \text{or} \quad \frac{\tilde{L}_2}{2} \leqslant \tilde{x} \leqslant \frac{\tilde{L}}{2} \tag{12}$$

$$\frac{\partial\theta}{\partial\tilde{y}} = 0 \quad \text{at} \quad \tilde{y} = \tilde{H} \quad \text{and} \quad -\frac{\tilde{L}}{2} \leqslant \tilde{x} \leqslant \frac{\tilde{L}}{2} \tag{13}$$

The boundary conditions on the cavity surfaces come from balancing the conduction and convection heat transfer, and their dimensionless resulting values are given by

$$-\frac{\partial\theta}{\partial\tilde{x}} = \frac{a^2}{2}\theta \quad \text{at} \quad \tilde{x} = -\frac{\tilde{L}_0}{2} \quad \text{or} \quad \tilde{x} = \frac{\tilde{L}_0}{2} \quad \text{and} \quad \tilde{H}_2 + \frac{\tilde{H}_1}{2} - \tilde{H}_0 \leqslant \tilde{y} \leqslant \tilde{H}_2 + \frac{\tilde{H}_1}{2} \tag{14}$$

$$-\frac{\partial\theta}{\partial\tilde{x}} = \frac{a^2}{2}\theta \quad \text{at} \quad \tilde{x} = -\tilde{L}_1 \quad \text{or} \quad \tilde{x} = \tilde{L}_1 \quad \text{and} \quad \tilde{H}_2 - \frac{\tilde{H}_1}{2} \leqslant \tilde{y} \leqslant \tilde{H}_2 + \frac{\tilde{H}_1}{2} \tag{15}$$

$$-\frac{\partial\theta}{\partial\tilde{x}} = \frac{a^2}{2}\theta \quad \text{at} \quad \tilde{x} = -\frac{\tilde{L}_2}{2} \quad \text{or} \quad \tilde{x} = \frac{\tilde{L}_2}{2} \quad \text{and} \quad 0 \leqslant \tilde{y} \leqslant \tilde{H}_2 - \frac{\tilde{H}_1}{2} \tag{16}$$

$$-\frac{\partial\theta}{\partial\tilde{y}} = \frac{a^2}{2}\theta \quad \text{at} \quad \tilde{y} = \tilde{H}_2 - \frac{\tilde{H}_1}{2} \quad \text{and} \quad -\tilde{L}_1 \leqslant \tilde{x} \leqslant -\frac{\tilde{L}_2}{2} \quad \text{or} \quad \frac{\tilde{L}_2}{2} \leqslant \tilde{x} \leqslant \tilde{L}_1 \tag{17}$$

$$-\frac{\partial\theta}{\partial\tilde{y}} = \frac{a^2}{2}\theta \quad \text{at} \quad \tilde{y} = \tilde{H}_2 + \frac{\tilde{H}_1}{2} \quad \text{and} \quad -\tilde{L}_1 \leqslant \tilde{x} \leqslant -\frac{\tilde{L}_0}{2} \quad \text{or} \quad \frac{\tilde{L}_0}{2} \leqslant \tilde{x} \leqslant \tilde{L}_1 \tag{18}$$

$$-\frac{\partial\theta}{\partial\tilde{y}} = \frac{a^2}{2}\theta \quad \text{at} \quad \tilde{y} = \tilde{H}_2 + \frac{\tilde{H}_1}{2} - \tilde{H}_0 \quad \text{and} \quad -\frac{\tilde{L}_0}{2} \leqslant \tilde{x} \leqslant \frac{\tilde{L}_0}{2} \tag{19}$$

The parameter (a) that emerged in Eqs. (14)–(19) was already used by Bejan and Almogbel [15] and defined as

$$a = \left(\frac{2hA^{1/2}}{k}\right)^{1/2} \tag{20}$$

The dimensionless form of Eqs. (1) and (5)–(7) are

$$1 = \tilde{H}\tilde{L} \tag{21}$$

$$\phi_c = (\tilde{H}_2 - \tilde{H}_1/2)\tilde{L}_2 + 2\tilde{L}_1\tilde{H}_1 - \phi_0 \tag{22}$$

$$\phi_0 = \tilde{H}_0\tilde{L}_0 \tag{23}$$

$$\psi = 2\tilde{L}_1\tilde{H}_2 + \tilde{L}_1\tilde{H}_1 \tag{24}$$

The maximal excess temperature, θ_{max}, is also the dimensionless global thermal resistance between the volume of the entire system (cavity and solid) and the surroundings

Table 1
Numerical tests showing the achievement of grid independence ($\phi_0 = 0.1$, $\phi_c = 0.2$, $\psi = 0.6$, $a = 0.1$, $H/L = 1$, $H_0/L_0 = 8.2$, $H_1/L_1 = 0.25$, $H_2/L_2 = 3$).

Number of elements	θ^i_{max}	$\lvert(\theta^i_{max} - \theta^{i+1}_{max})/\theta^i_{max}\rvert$
335	35.35115	3.6802×10^{-4}
1340	35.36416	1.4393×10^{-4}
5360	35.36925	5.4567×10^{-5}
21,440	35.37118	

Table 2
Comparison between the results obtained using our MATLAB partial-differential-equations (PDE) toolbox code ($\phi_c = 0.1$, $\phi_0 = 0.00001$, $\psi = 0.5$, $H/L = 1$, $H_0/L_0 = 1$, $H_1/L_1 = 0.036177$, $H_2/L_2 = 4.2524$) and the numerical results [12] ($D_0/D_1 = 0.1$, $L_0/L_1 = 0.65$).

	θ_{max}
This work	0.077402
Numerical [12]	0.076980

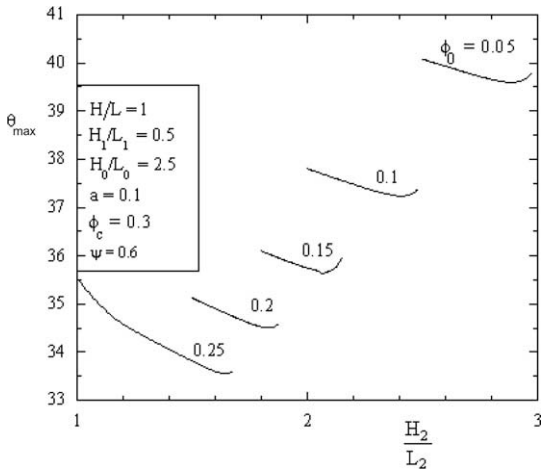

Fig. 2. Optimization of the global thermal resistance as function of H_2/L_2 for several values of the fraction of the area of the solid inserted into the cavity.

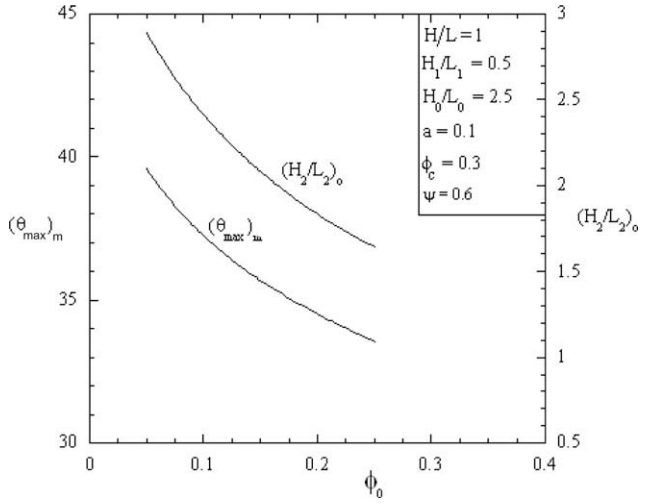

Fig. 3. The behavior of the once minimized global thermal resistance $(\theta_{max})_m$ and its corresponding optimal $(H_2/L_2)_o$ as function of ϕ_0.

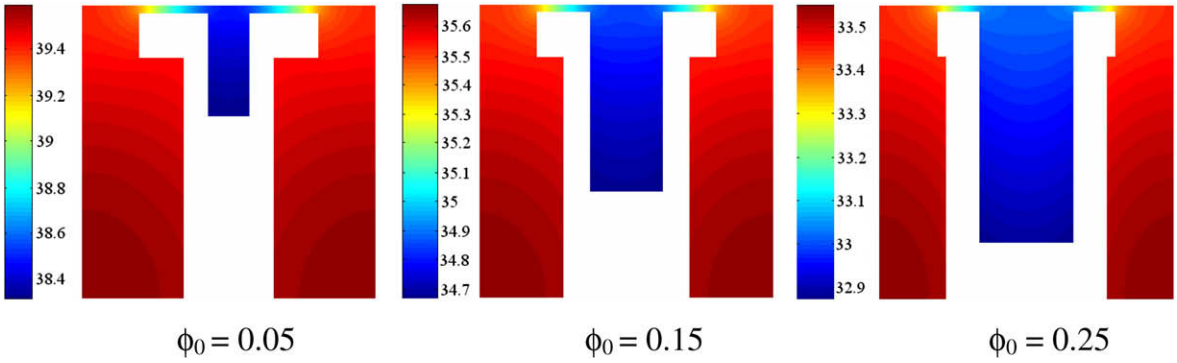

Fig. 4. Illustration of some optimal shapes from Fig. 3.

$$\theta_{max} = \frac{T_{max} - T_\infty}{q''' A/k} \tag{25}$$

3. Numerical model

The function defined by Eq. (25) can be determined numerically, by solving Eq. (8) for the temperature field in every assumed configuration (H/L, H_0/L_0, H_1/L_1, H_2/L_2), and calculating θ_{max} to see whether θ_{max} can be minimized by varying the configuration. In this sense, Eq. (8) was solved using a finite elements code, based on triangular elements, developed in MATLAB environment, precisely the PDE (partial-differential-equations) toolbox [16]. The grid was non-uniform in both $\tilde{x}$ and $\tilde{y}$, and varied from one geometry to the next. The appropriate mesh size was determined by successive refinements, increasing the number of elements four times from the current mesh size to the next mesh size, until the criterion $|(\theta^j_{max} - \theta^{j+1}_{max})/\theta^j_{max}| < 1 \times 10^{-4}$ was satisfied. Here, θ^j_{max} represents the maximum temperature calculated using the current mesh size, and θ^{j+1}_{max} corresponds to the maximum temperature using the next mesh, where the number of elements was increased by four times. Table 1 gives an example of how grid independence was achieved. The following results were performed by using a range between 2000 and 10,000 triangular elements.

To test the accuracy of the numerical code, the numerical results obtained using our code in Matlab PDE have been compared with the numerical results obtained by Biserni et al. [12]. The domain in this case was a T-shaped assembly of fins ($\phi_0 \approx 0$) and the boundary conditions were isothermal cavity surfaces, $\theta = 0$, and isolated outer surfaces. Table 2 shows that the two sets of results agree within 0.5%.

4. Optimal geometry

The numerical work consisted of determining the temperature field in a large number of configurations of the type shown in Fig. 1. Fig. 2 shows that there is an optimal ratio H_2/L_2 that minimizes the global thermal resistance when the parameters (ϕ_0, ϕ_c, ψ and a) and the degrees of freedom (H/L, H_1/L_1 and H_0/L_0) are fixed. Note that we used the value $a = 0.1$ in all the simulations because Bejan and Almogbel [15] illustrated an example of application to forced convection showing that, in order of magnitude sense, this number agrees with practical values used by industry.

Fig. 2 also shows the optimization of the global thermal resistance, θ_{max}, for several values of the fraction of the area of the solid inserted into the cavity, ϕ_0. The results of Fig. 2 were summarized in Fig. 3, which presents the once minimized global thermal resistance, $\theta_{max,m}$, and the once optimized ratio $(H_2/L_2)_o$, as function of the area of the solid inserted into the cavity fraction, ϕ_0. This figure indicates that $\theta_{max,m}$ and $(H_2/L_2)_o$ decrease when ϕ_0 increases. The best shapes calculated in Fig. 3 are shown in Fig. 4. This figure

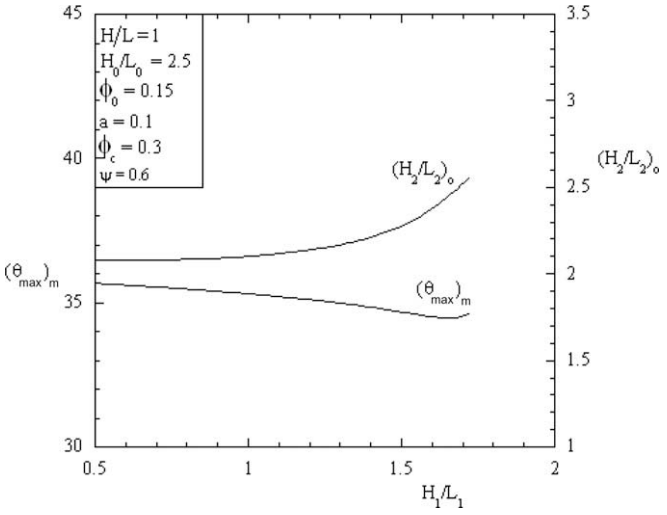

Fig. 5. Second optimization of the once optimized global thermal resistance and the corresponding optimal shape $(H_2/L_2)_o$ as function of the ration H_1/L_1.

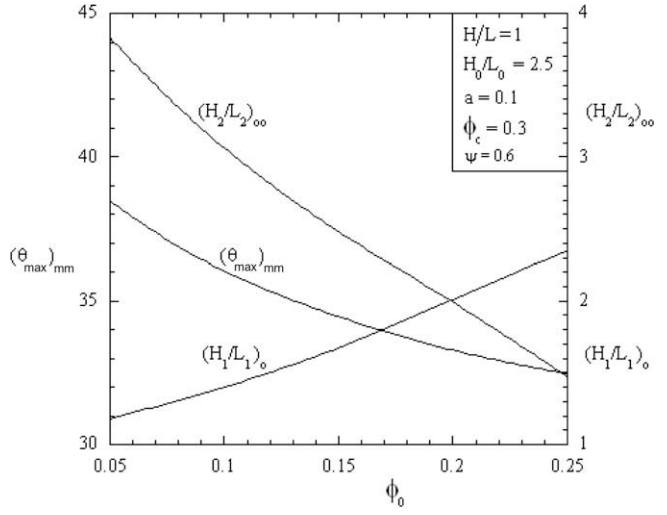

Fig. 6. The behavior of the twice optimized global thermal resistance, $(\theta_{max})_{mm}$, optimal ratios $(H_2/L_2)_{oo}$ and $(H_1/L_1)_o$ as function of ϕ_0.

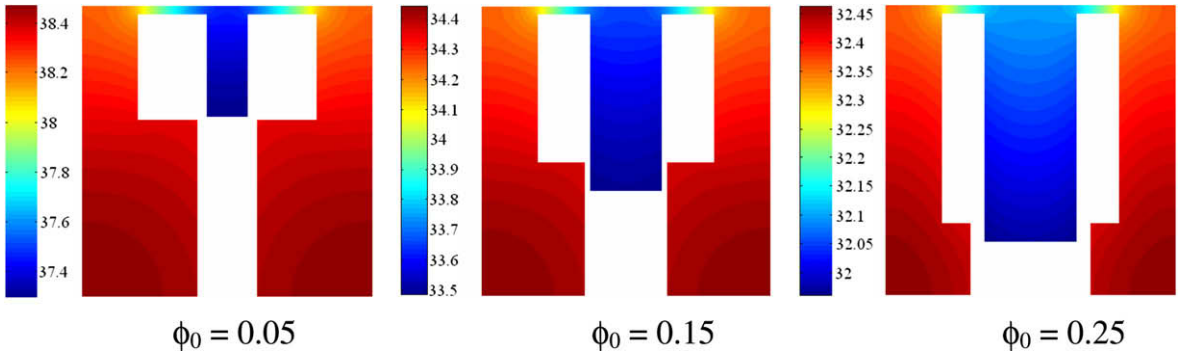

Fig. 7. The best shapes generated in Fig. 6.

confirms that cavities perform better when they penetrate almost completely into the body [12–14].

The procedure to obtain the minimal overall thermal resistance used in Figs. 2 and 3 is repeated in Fig. 5 for several values of the second degree of freedom, the ratio H_1/L_1, for a fixed $\phi_0 = 0.15$. This second optimization shows that there is a second minimum. Fig. 5 also shows that the corresponding $(H_2/L_2)_o$ value increases when the ratio H_1/L_1 also increases. The second optimization is also performed for several values of ϕ_0 and the results were presented in Fig. 6. This figure shows that the optimal ratio $(H_1/L_1)_o$ increases, while the optimal ratio $(H_2/L_2)_{oo}$ and the minimal thermal resistance, $\theta_{max,mm}$, both optimized twice decrease when ϕ_0 increases. The best shapes optimized twice in Fig. 6 were shown in Fig. 7 for several values of ϕ_0.

The third degree of freedom (H_0/L_0), according to Eq. (23), depends only on the parameter ϕ_0. Therefore, we used the optimal values obtained in Fig. 6 to perform the third optimization in Fig. 8. This figure shows that the twice optimized thermal resistance decreases when the third degree of freedom, H_0/L_0, increases for all the values of the parameter ϕ_0. The dashed line in Fig. 8 shows the value of the global thermal resistance for the largest allowed value for the ratio H_0/L_0, therefore the area of the solid inserted into the cavity penetrates completely into the cavity and reaches the coordinate $\tilde{y} = 0$. This dashed line also indicates that there is a minimum global thermal resistance as function of the parameter ϕ_0. This optimal value is shown in Fig. 9 where the three times minimized overall thermal resistance, $\theta_{max,mmm}$, and its corresponding optimal ratios $(H_2/L_2)_{ooo}$, $(H_1/L_1)_{oo}$ and $(H_o/L)_o$ are plotted against the area of the solid inserted into the cavity fraction, ϕ_0.

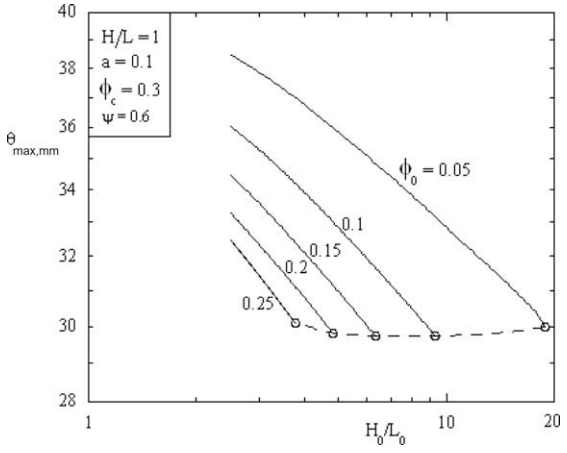

Fig. 8. Third optimization of the global thermal resistance as function of the ratio H_0/L_0 for several values of the parameter ϕ_0.

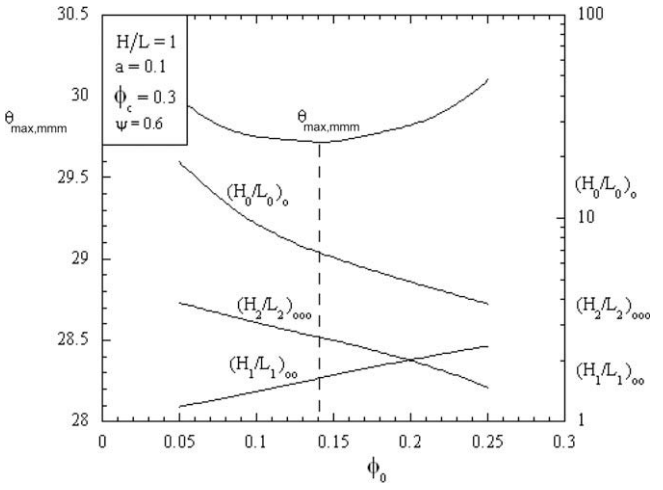

Fig. 9. Forth optimization: minimization of the global thermal resistance as a function of the parameter ϕ_0.

The optimal design has the following optimal ratios: $(H_2/L_2)_{ooo} = 2.61$, $(H_1/L_1)_{oo} = 1.63$ and $(H_0/L_0)_o = 6.77$.

Finally, the best configuration of Fig. 9 is compared with the best configuration calculated for the C-shaped cavity in Fig. 10. This figure was accomplished under the same thermal conditions and the same area of the cavity, i.e. Eqs. (8)–(10), appropriate boundary conditions and Eq. (22) do apply, but Eq. (22) is replaced by Eq. (26)

$$\phi_0 = \tilde{H}_c \tilde{L}_c \tag{26}$$

where $\tilde{H}_c$ is the height and $\tilde{L}_c$ is the length of the C-shaped cavity. The comparison shows that the T-Y-shaped cavity performs approximately 108% better than the C-shaped intrusion. This result was expected: according to Constructal theory geometric complexity, i.e. more freedom to morph [3], can increase the performance of the system.

5. Conclusions

This work applies Constructal design method to perform the optimization of the global thermal resistance of a T-Y-shaped cavity.

The results show that there is an optimal shape of the cavity that minimizes the global thermal resistance when the total volume and the cavity volume are fixed. This configuration is achieved when the cavity penetrates almost completely in the body, the shape of the area of the solid inserted into the cavity is long enough

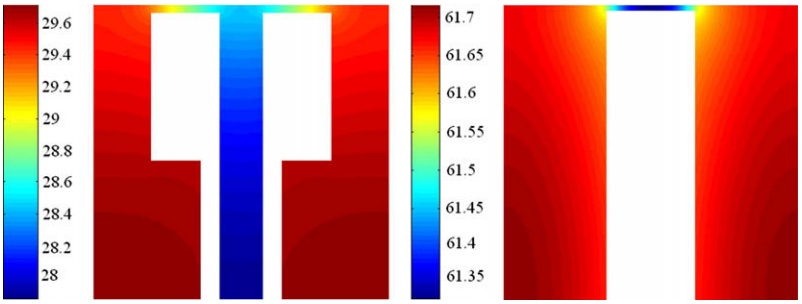

Fig. 10. Comparison between the best shape of Fig. 9 and the best C-shaped cavity.

to cross completely the T-Y cavity (ending at the coordinate $\tilde{y} \cong 0$), and this area is 14% of the total area occupied by the body and the T-Y-shaped cavity.

When compared with the C-shaped cavity under the same thermal conditions and the same area of the cavity, the T-Y-shaped cavity is approximately 108% superior.

Our results agree with former studies that show that the cavity performs better when it penetrates almost completely into the body. They also confirm that geometric complexity can improve the performance of the flow system.

This study also deserves further investigation in the future; therefore, we will learn the effect on the global thermal resistance of the area of cavity, the aspect ratio of the body, and the parameters 'a' and ψ that were not addressed in this paper.

Acknowledgements

Prof. Giulio Lorenzini's work was sponsored by the Italian Ministry for Education, University and Research.

Prof. Luiz Rocha's work was sponsored by FAPERGS, Porto Alegre, RS, Brazil.

References

[1] A. Bejan, Advanced Engineering Thermodynamics, second ed., Wiley, New York, 1997.
[2] A. Bejan, Shape and Structure, from Engineering to Nature, Cambridge University Press, Cambridge, UK, 2000.
[3] A. Bejan, S. Lorente, Design with Constructal Theory, Wiley, Hoboken, 2008.
[4] A. Bejan, S. Lorente, Constructal theory of generation of configuration in nature and engineering, J. Appl. Phys. 100 (2006) 041301.
[5] A.D. Kraus, Developments in the analysis of finned arrays, Donald Q. Kern Award Lecture, National Heat Transfer Conference, Baltimore, MD, August 11, 1997, Int. J. Transport Phenomena 1 (1999) 141–164.
[6] A. Aziz, Optimum dimensions of extended surfaces operating in a convective environment, Appl. Mech. Rev. 45 (5) (1992) 155–173.
[7] H.D. Falter, E. Thompson, Performance of hypervapotron beamstopping elements at jet, Fusion Technol. 29 (1996) 584–594.
[8] C. Biserni, G. Lorenzini, Experimental tests on subcooled boiling heat transfer under forced convection conditions, J. Eng. Thermophys. 11 (2002) 73–81.
[9] G. Lorenzini, C. Biserni, A Vapotron effect application for electronic equipment cooling, J. Electron. Packaging 125 (2003) 475–479.
[10] G. Lorenzini, L.A.O. Rocha, Constructal design of Y-shaped assembly of fins, Int. J. Heat Mass Transfer 49 (2006) 4552–4557.
[11] G. Lorenzini, L.A.O. Rocha, Constructal design of T-Y assembly of fins for an optimal heat removal, Int. J. Heat Mass Transfer 52 (2009) 1458–1463.
[12] C. Biserni, L.A.O. Rocha, A. Bejan, Inverted fins: geometric optimization of the intrusion into a conducting wall, Int. J. Heat Mass Transfer 47 (2004) 2577–2586.
[13] L.A.O. Rocha, E. Lorenzini, C. Biserni, Geometric optimization of shapes on the basis of Bejan's Constructal theory, Int. Commun. Heat Mass Transfer 32 (2005) 1281–1288.
[14] C. Biserni, L.A.O. Rocha, G. Stanescu, E. Lorenzini, Constructal H-shaped cavities according to Bejan's theory, Int. J. Heat Mass Transfer 50 (2007) 2132–2138.
[15] A. Bejan, M. Almogbel, Constructal T-shaped fins, Int. J. Heat Mass Transfer 43 (2000) 2101–2115.
[16] MATLAB, User's Guide, Version 6.0.088, Release 12, The Mathworks Inc., 2000.